Measurement of the cross section for prompt isolated diphoton production using the full CDF Run II data sample

T. Aaltonen,[21] S. Amerio,[40] D. Amidei,[32] A. Anastassov[x],[15] A. Annovi,[17] J. Antos,[12] G. Apollinari,[15] J.A. Appel,[15] T. Arisawa,[53] A. Artikov,[13] J. Asaadi,[48] W. Ashmanskas,[15] B. Auerbach,[2] A. Aurisano,[48] F. Azfar,[39] W. Badgett,[15] T. Bae,[25] A. Barbaro-Galtieri,[26] V.E. Barnes,[44] B.A. Barnett,[23] P. Barria[hh],[42] P. Bartos,[12] M. Bauce[ff],[40] F. Bedeschi,[42] S. Behari,[15] G. Bellettini[gg],[42] J. Bellinger,[55] D. Benjamin,[14] A. Beretvas,[15] A. Bhatti,[46] K.R. Bland,[5] B. Blumenfeld,[23] A. Bocci,[14] A. Bodek,[45] D. Bortoletto,[44] J. Boudreau,[43] A. Boveia,[11] L. Brigliadori[ee],[6] C. Bromberg,[33] E. Brucken,[21] J. Budagov,[13] H.S. Budd,[45] K. Burkett,[15] G. Busetto[ff],[40] P. Bussey,[19] P. Butti[gg],[42] A. Buzatu,[19] A. Calamba,[10] S. Camarda,[4] M. Campanelli,[28] F. Canelli[oo],[11,15] B. Carls,[22] D. Carlsmith,[55] R. Carosi,[42] S. Carrillo[m],[16] B. Casal[k],[9] M. Casarsa,[49] A. Castro[ee],[6] P. Catastini,[20] D. Cauz,[49] V. Cavaliere,[22] M. Cavalli-Sforza,[4] A. Cerri[f],[26] L. Cerrito[s],[28] Y.C. Chen,[1] M. Chertok,[7] G. Chiarelli,[42] G. Chlachidze,[15] K. Cho,[25] D. Chokheli,[13] M.A. Ciocci[hh],[42] A. Clark,[18] C. Clarke,[54] M.E. Convery,[15] J. Conway,[7] M .Corbo,[15] M. Cordelli,[17] C.A. Cox,[7] D.J. Cox,[7] M. Cremonesi,[42] D. Cruz,[48] J. Cuevas[z],[9] R. Culbertson,[15] N. d'Ascenzo[w],[15] M. Datta[qq],[15] P. De Barbaro,[45] L. Demortier,[46] M. Deninno,[6] F. Devoto,[21] M. d'Errico[ff],[40] A. Di Canto[gg],[42] B. Di Ruzza[q],[15] J.R. Dittmann,[5] M. D'Onofrio,[27] S. Donati[gg],[42] M. Dorigo[nn],[49] A. Driutti,[49] K. Ebina,[53] R. Edgar,[32] A. Elagin,[48] R. Erbacher,[7] S. Errede,[22] B. Esham,[22] R. Eusebi,[48] S. Farrington,[39] J.P. Fernández Ramos,[29] R. Field,[16] G. Flanagan[u],[15] R. Forrest,[7] M. Franklin,[20] J.C. Freeman,[15] H. Frisch,[11] Y. Funakoshi,[53] A.F. Garfinkel,[44] P. Garosi[hh],[42] H. Gerberich,[22] E. Gerchtein,[15] S. Giagu,[47] V. Giakoumopoulou,[3] K. Gibson,[43] C.M. Ginsburg,[15] N. Giokaris,[3] P. Giromini,[17] G. Giurgiu,[23] V. Glagolev,[13] D. Glenzinski,[15] M. Gold,[35] D. Goldin,[48] A. Golossanov,[15] G. Gomez,[9] G. Gomez-Ceballos,[30] M. Goncharov,[30] O. González López,[29] I. Gorelov,[35] A.T. Goshaw,[14] K. Goulianos,[46] E. Gramellini,[6] S. Grinstein,[4] C. Grosso-Pilcher,[11] R.C. Group[52],[15] J. Guimaraes da Costa,[20] S.R. Hahn,[15] J.Y. Han,[45] F. Happacher,[17] K. Hara,[50] M. Hare,[51] R.F. Harr,[54] T. Harrington-Taber[n],[15] K. Hatakeyama,[5] C. Hays,[39] J. Heinrich,[41] M. Herndon,[55] A. Hocker,[15] Z. Hong,[48] W. Hopkins[g],[15] S. Hou,[1] R.E. Hughes,[36] U. Husemann,[56] J. Huston,[33] G. Introzzi[mm],[42] M. Iori[jj],[47] A. Ivanov[p],[7] E. James,[15] D. Jang,[10] B. Jayatilaka,[15] E.J. Jeon,[25] S. Jindariani,[15] M. Jones,[44] K.K. Joo,[25] S.Y. Jun,[10] T.R. Junk,[15] M. Kambeitz,[24] T. Kamon[25,48] P.E. Karchin,[54] A. Kasmi,[5] Y. Kato[o],[38] W. Ketchum[rr],[11] J. Keung,[41] B. Kilminster[oo],[15] D.H. Kim,[25] H.S. Kim,[25] J.E. Kim,[25] M.J. Kim,[17] S.B. Kim,[25] S.H. Kim,[50] Y.K. Kim,[11] Y.J. Kim,[25] N. Kimura,[53] M. Kirby,[15] K. Knoepfel,[15] K. Kondo*,[53] D.J. Kong,[25] J. Konigsberg,[16] A.V. Kotwal,[14] M. Kreps,[24] J. Kroll,[41] M. Kruse,[14] T. Kuhr,[24] M. Kurata,[50] A.T. Laasanen,[44] S. Lammel,[15] M. Lancaster,[28] K. Lannon[y],[36] G. Latino[hh],[42] H.S. Lee,[25] J.S. Lee,[25] S. Leo,[42] S. Leone,[42] J.D. Lewis,[15] A. Limosani[t],[14] E. Lipeles,[41] H. Liu,[52] Q. Liu,[44] T. Liu,[15] S. Lockwitz,[56] A. Loginov,[56] D. Lucchesi[ff],[40] J. Lueck,[24] P. Lujan,[26] P. Lukens,[15] G. Lungu,[46] J. Lys,[26] R. Lysak[e],[12] R. Madrak,[15] P. Maestro[hh],[42] S. Malik,[46] G. Manca[a],[27] A. Manousakis-Katsikakis,[3] F. Margaroli,[47] P. Marino[ii],[42] M. Martínez,[4] K. Matera,[22] M.E. Mattson,[54] A. Mazzacane,[15] P. Mazzanti,[6] R. McNulty[j],[27] A. Mehta,[27] P. Mehtala,[21] C. Mesropian,[46] T. Miao,[15] D. Mietlicki,[32] A. Mitra,[1] H. Miyake,[50] S. Moed,[15] N. Moggi,[6] C.S. Moon,[25] R. Moore[pp],[15] M.J. Morello[ii],[42] A. Mukherjee,[15] Th. Muller,[24] P. Murat,[15] M. Mussini[ee],[6] J. Nachtman[n],[15] Y. Nagai,[50] J. Naganoma,[53] I. Nakano,[37] A. Napier,[51] J. Nett,[48] C. Neu,[52] T. Nigmanov,[43] L. Nodulman,[2] S.Y. Noh,[25] O. Norniella,[22] L. Oakes,[39] S.H. Oh,[14] Y.D. Oh,[25] I. Oksuzian,[52] T. Okusawa,[38] R. Orava,[21] L. Ortolan,[4] C. Pagliarone,[49] E. Palencia[f],[9] P. Palni,[35] V. Papadimitriou,[15] W. Parker,[55] G. Pauletta[kk],[49] M. Paulini,[10] C. Paus,[30] T.J. Phillips,[14] G. Piacentino,[42] E. Pianori,[41] J. Pilot,[36] K. Pitts,[22] C. Plager,[8] L. Pondrom,[55] S. Poprocki[g],[15] K. Potamianos,[26] F. Prokoshin[cc],[13] A. Pranko,[26] F. Ptohos[h],[17] G. Punzi[gg],[42] N. Ranjan,[44] I. Redondo Fernández,[29] P. Renton,[39] M. Rescigno,[47] T. Riddick,[28] F. Rimondi*,[6] L. Ristori[42],[15] A. Robson,[19] T. Rodriguez,[41] S. Rolli[i],[51] M. Ronzani[gg],[42] R. Roser,[15] J.L. Rosner,[11] F. Ruffini[hh],[42] A. Ruiz,[9] J. Russ,[10] V. Rusu,[15] A. Safonov,[48] W.K. Sakumoto,[45] Y. Sakurai,[53] L. Santi[kk],[49] K. Sato,[50] V. Saveliev[w],[15] A. Savoy-Navarro[aa],[15] P. Schlabach,[15] E.E. Schmidt,[15] T. Schwarz,[32] L. Scodellaro,[9] F. Scuri,[42] S. Seidel,[35] Y. Seiya,[38] A. Semenov,[13] F. Sforza[gg],[42] S.Z. Shalhout,[7] T. Shears,[27] P.F. Shepard,[43] M. Shimojima[v],[50] M. Shochet,[11] I. Shreyber-Tecker,[34] A. Simonenko,[13] P. Sinervo,[31] K. Sliwa,[51] J.R. Smith,[7] F.D. Snider,[15] V. Sorin,[4] H. Song,[43] M. Stancari,[15] R. St. Denis,[19] B. Stelzer,[31] O. Stelzer-Chilton,[31] D. Stentz[x],[15] J. Strologas,[35] Y. Sudo,[50] A. Sukhanov,[15] I. Suslov,[13] K. Takemasa,[50] Y. Takeuchi,[50] J. Tang,[11] M. Tecchio,[32] P.K. Teng,[1] J. Thom[g],[15] E. Thomson,[41] V. Thukral,[48] D. Toback,[48] S. Tokar,[12] K. Tollefson,[33] T. Tomura,[50] D. Tonelli[f],[15] S. Torre,[17] D. Torretta,[15] P. Totaro,[40] M. Trovato[ii],[42] F. Ukegawa,[50] S. Uozumi,[25] F. Vázquez[m],[16] G. Velev,[15] C. Vellidis,[15]

C. Vernieri[ii],[42] M. Vidal,[44] R. Vilar,[9] J. Vizán[ll],[9] M. Vogel,[35] G. Volpi,[17] P. Wagner,[41] R. Wallny,[8] S.M. Wang,[1] A. Warburton,[31] D. Waters,[28] W.C. Wester III,[15] D. Whiteson[b],[41] A.B. Wicklund,[2] S. Wilbur,[11] H.H. Williams,[41] J.S. Wilson,[32] P. Wilson,[15] B.L. Winer,[36] P. Wittich[g],[15] S. Wolbers,[15] H. Wolfe,[36] T. Wright,[32] X. Wu,[18] Z. Wu,[5] K. Yamamoto,[38] D. Yamato,[38] T. Yang,[15] U.K. Yang[r],[11] Y.C. Yang,[25] W.-M. Yao,[26] G.P. Yeh,[15] K. Yi[n],[15] J. Yoh,[15] K. Yorita,[53] T. Yoshida[l],[38] G.B. Yu,[14] I. Yu,[25] A.M. Zanetti,[49] Y. Zeng,[14] C. Zhou,[14] and S. Zucchelli[ee6]

(CDF Collaboration[†])

[1]*Institute of Physics, Academia Sinica, Taipei, Taiwan 11529, Republic of China*
[2]*Argonne National Laboratory, Argonne, Illinois 60439, USA*
[3]*University of Athens, 157 71 Athens, Greece*
[4]*Institut de Fisica d'Altes Energies, ICREA, Universitat Autonoma de Barcelona, E-08193, Bellaterra (Barcelona), Spain*
[5]*Baylor University, Waco, Texas 76798, USA*
[6]*Istituto Nazionale di Fisica Nucleare Bologna, [ee]University of Bologna, I-40127 Bologna, Italy*
[7]*University of California, Davis, Davis, California 95616, USA*
[8]*University of California, Los Angeles, Los Angeles, California 90024, USA*
[9]*Instituto de Fisica de Cantabria, CSIC-University of Cantabria, 39005 Santander, Spain*
[10]*Carnegie Mellon University, Pittsburgh, Pennsylvania 15213, USA*
[11]*Enrico Fermi Institute, University of Chicago, Chicago, Illinois 60637, USA*
[12]*Comenius University, 842 48 Bratislava, Slovakia; Institute of Experimental Physics, 040 01 Kosice, Slovakia*
[13]*Joint Institute for Nuclear Research, RU-141980 Dubna, Russia*
[14]*Duke University, Durham, North Carolina 27708, USA*
[15]*Fermi National Accelerator Laboratory, Batavia, Illinois 60510, USA*
[16]*University of Florida, Gainesville, Florida 32611, USA*
[17]*Laboratori Nazionali di Frascati, Istituto Nazionale di Fisica Nucleare, I-00044 Frascati, Italy*
[18]*University of Geneva, CH-1211 Geneva 4, Switzerland*
[19]*Glasgow University, Glasgow G12 8QQ, United Kingdom*
[20]*Harvard University, Cambridge, Massachusetts 02138, USA*
[21]*Division of High Energy Physics, Department of Physics,*
University of Helsinki and Helsinki Institute of Physics, FIN-00014, Helsinki, Finland
[22]*University of Illinois, Urbana, Illinois 61801, USA*
[23]*The Johns Hopkins University, Baltimore, Maryland 21218, USA*
[24]*Institut für Experimentelle Kernphysik, Karlsruhe Institute of Technology, D-76131 Karlsruhe, Germany*
[25]*Center for High Energy Physics: Kyungpook National University,*
Daegu 702-701, Korea; Seoul National University, Seoul 151-742,
Korea; Sungkyunkwan University, Suwon 440-746,
Korea; Korea Institute of Science and Technology Information,
Daejeon 305-806, Korea; Chonnam National University,
Gwangju 500-757, Korea; Chonbuk National University, Jeonju 561-756,
Korea; Ewha Womans University, Seoul, 120-750, Korea
[26]*Ernest Orlando Lawrence Berkeley National Laboratory, Berkeley, California 94720, USA*
[27]*University of Liverpool, Liverpool L69 7ZE, United Kingdom*
[28]*University College London, London WC1E 6BT, United Kingdom*
[29]*Centro de Investigaciones Energeticas Medioambientales y Tecnologicas, E-28040 Madrid, Spain*
[30]*Massachusetts Institute of Technology, Cambridge, Massachusetts 02139, USA*
[31]*Institute of Particle Physics: McGill University, Montréal, Québec H3A 2T8,*
Canada; Simon Fraser University, Burnaby, British Columbia V5A 1S6,
Canada; University of Toronto, Toronto, Ontario M5S 1A7,
Canada; and TRIUMF, Vancouver, British Columbia V6T 2A3, Canada
[32]*University of Michigan, Ann Arbor, Michigan 48109, USA*
[33]*Michigan State University, East Lansing, Michigan 48824, USA*
[34]*Institution for Theoretical and Experimental Physics, ITEP, Moscow 117259, Russia*
[35]*University of New Mexico, Albuquerque, New Mexico 87131, USA*
[36]*The Ohio State University, Columbus, Ohio 43210, USA*
[37]*Okayama University, Okayama 700-8530, Japan*
[38]*Osaka City University, Osaka 588, Japan*
[39]*University of Oxford, Oxford OX1 3RH, United Kingdom*
[40]*Istituto Nazionale di Fisica Nucleare, Sezione di Padova-Trento, [ff]University of Padova, I-35131 Padova, Italy*
[41]*University of Pennsylvania, Philadelphia, Pennsylvania 19104, USA*
[42]*Istituto Nazionale di Fisica Nucleare Pisa, [gg]University of Pisa,*
[hh]*University of Siena and [ii]Scuola Normale Superiore, I-56127 Pisa,*
Italy, [mm]INFN Pavia and University of Pavia, I-27100 Pavia, Italy
[43]*University of Pittsburgh, Pittsburgh, Pennsylvania 15260, USA*
[44]*Purdue University, West Lafayette, Indiana 47907, USA*

[45] *University of Rochester, Rochester, New York 14627, USA*
[46] *The Rockefeller University, New York, New York 10065, USA*
[47] *Istituto Nazionale di Fisica Nucleare, Sezione di Roma 1,*
[jj] *Sapienza Università di Roma, I-00185 Roma, Italy*
[48] *Texas A&M University, College Station, Texas 77843, USA*
[49] *Istituto Nazionale di Fisica Nucleare Trieste/Udine;* [nn] *University of Trieste,*
I-34127 Trieste, Italy; [kk] *University of Udine, I-33100 Udine, Italy*
[50] *University of Tsukuba, Tsukuba, Ibaraki 305, Japan*
[51] *Tufts University, Medford, Massachusetts 02155, USA*
[52] *University of Virginia, Charlottesville, Virginia 22906, USA*
[53] *Waseda University, Tokyo 169, Japan*
[54] *Wayne State University, Detroit, Michigan 48201, USA*
[55] *University of Wisconsin, Madison, Wisconsin 53706, USA*
[56] *Yale University, New Haven, Connecticut 06520, USA*
(Dated: December 13, 2012)

This Letter reports a measurement of the cross section for producing pairs of central prompt isolated photons in proton-antiproton collisions at a total energy $\sqrt{s} = 1.96$ TeV using data corresponding to 9.5 fb^{-1} integrated luminosity collected with the CDF II detector at the Fermilab Tevatron. The measured differential cross section is compared to three calculations derived from the theory of strong interactions. These include a prediction based on a leading order matrix element calculation merged with parton shower, a next-to-leading order, and a next-to-next-to-leading order calculation. The first and last calculations reproduce most aspects of the data, thus showing the importance of higher-order contributions for understanding the theory of strong interaction and improving measurements of the Higgs boson and searches for new phenomena in diphoton final states.

The production of prompt photon pairs in hadron col-

––––––––

[*]Deceased

[†]With visitors from [a]Istituto Nazionale di Fisica Nucleare, Sezione di Cagliari, 09042 Monserrato (Cagliari), Italy, [b]University of California Irvine, Irvine, CA 92697, USA, [c]University of California Santa Barbara, Santa Barbara, CA 93106, USA, [d]University of California Santa Cruz, Santa Cruz, CA 95064, USA, [e]Institute of Physics, Academy of Sciences of the Czech Republic, 182 21, Czech Republic, [f]CERN, CH-1211 Geneva, Switzerland, [g]Cornell University, Ithaca, NY 14853, USA, [h]University of Cyprus, Nicosia CY-1678, Cyprus, [i]Office of Science, U.S. Department of Energy, Washington, DC 20585, USA, [j]University College Dublin, Dublin 4, Ireland, [k]ETH, 8092 Zürich, Switzerland, [l]University of Fukui, Fukui City, Fukui Prefecture, Japan 910-0017, [m]Universidad Iberoamericana, Lomas de Santa Fe, México, C.P. 01219, Distrito Federal, [n]University of Iowa, Iowa City, IA 52242, USA, [o]Kinki University, Higashi-Osaka City, Japan 577-8502, [p]Kansas State University, Manhattan, KS 66506, USA, [q]Brookhaven National Laboratory, Upton, NY 11973, USA, [r]University of Manchester, Manchester M13 9PL, United Kingdom, [s]Queen Mary, University of London, London, E1 4NS, United Kingdom, [t]University of Melbourne, Victoria 3010, Australia, [u]Muons, Inc., Batavia, IL 60510, USA, [v]Nagasaki Institute of Applied Science, Nagasaki 851-0193, Japan, [w]National Research Nuclear University, Moscow 115409, Russia, [x]Northwestern University, Evanston, IL 60208, USA, [y]University of Notre Dame, Notre Dame, IN 46556, USA, [z]Universidad de Oviedo, E-33007 Oviedo, Spain, [aa]CNRS-IN2P3, Paris, F-75205 France, [bb]Texas Tech University, Lubbock, TX 79609, USA, [cc]Universidad Tecnica Federico Santa Maria, 110v Valparaiso, Chile, [dd]Yarmouk University, Irbid 211-63, Jordan, [ll]Universite catholique de Louvain, 1348 Louvain-La-Neuve, Belgium, [oo]University of Zürich, 8006 Zürich, Switzerland, [pp]Massachusetts General Hospital and Harvard Medical School, Boston, MA 02114 USA, [qq]Hampton University, Hampton, VA 23668, USA, [rr]Los Alamos National Laboratory, Los Alamos, NM 87544, USA

lisions is a significant, irreducible background in searches for a low-mass Higgs boson decaying into a photon pair [1], as well as in searches for new phenomena, such as extra spatial dimensions [2–4] and two-body [5] or cascade [6] decays of new heavy particles. Precise measurements of the production cross sections for diphotons as functions of various kinematic variables and their theoretical understanding are important for these searches. The better the prompt diphoton background is understood, the smaller uncertainties are introduced in these searches. After the recent discovery of the Higgs boson-like particle at the LHC [7], a better understanding of the background is important for improvements in the precision of the measurements of the production cross section and the decay branching ratio of this particle into a photon pair. A precise measurement of the branching ratio is of special importance, as this decay proceeds through a fermion loop and thus it indirectly constrains the couplings of the Higgs boson-like particle to fermions, which are more difficult to extract from direct decays into fermion pairs. Diphoton production is also used to test quantum chromodynamics (QCD), the theory of strong interaction, both in the perturbative scheme (pQCD), which is a good approximation at high energies, and in non-perturbative schemes, such as soft-gluon resummation methods, which provide important corrections in certain lower-energy kinematic regions [8]. Diphotons are expected to be dominantly produced by quark-antiquark annihilation $q\bar{q} \to \gamma\gamma$ and, in kinematic regions where gluons dominate the parton distribution functions (PDF), by gluon-gluon fusion $gg \to \gamma\gamma$ through a quark loop amplitude. Prompt photons may also result

from quark fragmentation in hard scattering, although a strict photon isolation requirement significantly reduces the fragmentation contributions.

Diphoton measurements have been made previously at fixed-target [9] and collider experiments [10–12]. Recent measurements have been made both at the Tevatron [13, 14] and at the LHC [15], which offer a consistent picture on the accuracy and limitations of the theoretical calculations in reproducing the data. The ATLAS measurement [15] found diphoton production features in proton-proton collisions at $\sqrt{s} = 7$ TeV analogous to those observed in proton-antiproton collisions at $\sqrt{s} = 1.96$ TeV [13, 14]. The most recent CDF measurement [14], using approximately half the full CDF data sample, compared the data with pQCD calculations at leading order (LO) and next-to-leading order (NLO) in the expansion parameter α_s, the strong interaction coupling. Large discrepancies were found between the data and a LO matrix-element calculation supplemented with a parton shower (PS) model. The inclusion of photons radiated from initial- and final-state quarks allowed by the shower model substantially improved the agreement of the PS calculation with the data. The calculation that includes radiated photons was recently used to predict the non-resonant background in the search for a low-mass Higgs boson decaying into a photon pair using the full CDF data set [16].

This work presents the final diphoton measurements from CDF using the full data set collected in 2001–2011 corresponding to a total integrated luminosity of 9.5 fb^{-1}. The results are compared with all the available state-of-the-art calculations under a variety of kinematic conditions [17], including an improved set of calculations not discussed in the previous work [14].

The reported measurement is using data collected with the Collider Detector at Fermilab (CDF) [18], at the Tevatron $p\bar{p}$ collider. The CDF detector includes a central spectrometer inside a 1.4 T axial magnetic field, surrounded by electromagnetic and hadronic calorimeters and muon detection chambers. The inner spectrometer measures charged particle trajectories (tracks) with a momentum component transverse to the beam (p_T) with a precision of $\sigma_{p_T}/p_T^2 = 0.07\%(\text{GeV}/c)^{-1}$. The pointing-tower-geometry central calorimeters cover the region $|\eta| < 1.1$, with an electromagnetic (hadronic) energy resolution of $\sigma(E_T)/E_T = 13.5\%/\sqrt{E_T(\text{GeV})} \oplus 1.5\%$ ($\sigma(E_T)/E_T = 50\%/\sqrt{E_T(\text{GeV})} \oplus 3\%$) and a tower segmentation of $\Delta\eta \times \Delta\phi \simeq 0.1 \times 15°$, where $E_T = E\sin\theta$ is the transverse energy, $\eta = -\ln[\tan(\theta/2)]$ is the pseudorapidity, θ is the polar angle and ϕ the azimuth of the tower's axis in the coordinate system of the laboratory, with polar axis along the proton beam direction and origin at the center of the detector. Photons are reconstructed in clusters of up to three towers [19] in the central calorimeter only. The pseudorapidity of each photon in the event is restricted to the region $|\eta| < 1$. A finely-segmented detector located at a depth corresponding to the maximum development of a typical electromagnetic shower measures the energy deposit profile, which is required to be consistent with originating from a single photon. The photon transverse energy is required to exceed 17 GeV for the first photon in the event and 15 GeV for the second photon. The transverse energy measured by the calorimeter in an isolation cone with radius in $\eta - \phi$ space of 0.4 around each photon [20] is required not to exceed 2 GeV.

This measurement employs the same techniques as the previous work [14]. Inclusive diphoton events are selected online by requiring two isolated electromagnetic clusters with $E_T > 12$ GeV each or two electromagnetic clusters with $E_T > 18$ GeV and no isolation requirement. In the offline analysis additional requirements are imposed to identify a sample rich in prompt photons. The background from events where one or both reconstructed photons are misidentified jets is subtracted with a 4×4 matrix technique using the track isolation as the discriminant between signal and background [21]. The matrix is constructed for each event from the E_T-dependent efficiencies of signal and background photons passing the track isolation criterion. This technique takes into account the full correlations between the two photons in the event. An optimal track-isolation threshold of 1 GeV/c is determined by maximizing the discrimination between signal and background Monte Carlo (MC) simulation samples. The efficiencies used in this method are determined from γ+jet and dijet samples generated with PYTHIA [22], subjected to the full detector and online event selection simulation [23], and reconstructed as the experimental data. The signal fraction is determined by summing the probabilities of an event to be pure signal, pure background, and a mixed photon pair. These probabilities are obtained for each event by multiplying the 4×4 matrix with the four-dimensional column vector of the observation values (0 or 1) for all four combinations of the first and second photon having track isolation larger or smaller than 1 GeV/c and inverting the result. The systematic uncertainty in the signal fraction is in the range of 15–20%.

The differential cross section for diphoton production is obtained from the histogram of the estimated signal yield as a function of each relevant kinematic variable. The average cross section in a bin is determined by dividing the yield by the product of the trigger efficiency, the selection efficiency and acceptance, the integrated luminosity, and the bin size. The diphoton trigger efficiency is derived from data [1]. It is consistent with 100% over all of the kinematic range with a flat uncertainty of 3%. The diphoton selection efficiency accounts for the effects from the *underlying event* from collision remnants [14] and from additional (pile-up) collisions overlapping with the collision that produced the photons. The systematic uncertainty in the selection efficiency related to the pile-

up effect grows linearly from 1.8% for $E_T \leq 40$ GeV to 3% for $E_T = 80$ GeV and remains constant above this point. A flat 3% uncertainty per photon accounts for possible inaccuracies in the PYTHIA model for the underlying event. This is summed linearly to 6% for two photons, since the underlying event is not related with prompt photon production and affects only the isolation in a way, on the average, symmetric for the two photons. A 6% constant uncertainty comes from the integrated luminosity [24]. The difference in the photon identification efficiency between data and MC is estimated from the $Z^0 \to e^+e^-$ sample [1] and added as a systematic uncertainty to the measurement. The electromagnetic energy scale is determined from the mass of the $Z^0 \to e^+e^-$ signal. The associated systematic uncertainty is estimated to grow linearly from 0 at $E_T \leq 40$ GeV up to 1.5% at $E_T = 80$ GeV and remain constant above this point. All systematic uncertainties are added in quadrature.

In the previous measurement [14], the experimental results were compared with three theoretical calculations: (i) the fixed NLO predictions of the DIPHOX program [25], including non-perturbative parton fragmentation into photons at NLO [26], (ii) the predictions of the RESBOS program [8] where the cross section is accurate to NLO, but also has an analytical initial-state soft-gluon resummation, and (iii) the predictions of the PYTHIA PS program [22] including photons radiated from initial- and final-state quarks [14]. Within their known limitations, all three calculations reproduced the main features of the data, but none of them described all aspects of the data. In this Letter, the measurement is compared with three different calculations: (a) the fixed NLO predictions of the MCFM program [27], including non-perturbative parton fragmentation into photons at LO [28], (b) the fixed next-to-next-to-leading order (NNLO) predictions of a recent calculation [29], and (c) the predictions of the SHERPA program [30], based on a matrix element calculation merged with parton shower (ME+PS). This calculation features a realistic representation of the physics events including initial- and final-state radiation. The prediction of MCFM is an alternative calculation to DIPHOX, but it has not been tested against any previous measurement. The NNLO and SHERPA predictions are recent calculations that are expected to reproduce the data features better than the previous calculations.

While the NLO and NNLO matrix elements for diphoton production include all real and virtual processes at fixed order in α_s, the SHERPA matrix element includes only real processes at NNLO. However, by merging the matrix element contribution (the hard scattering process) with those from the parton shower (cascade radiation subprocesses from the initial- and final-state quarks and gluons), this calculation accounts for real processes effectively at all orders in α_s. It also accounts for some virtual effects via corrections applied in the parton shower subprocesses. The SHERPA calculation is an extension of the PYTHIA calculation including photons radiated from initial- and final-state quarks which was introduced in the previous measurement [14]. In the default SHERPA calculation the scale is adjusted to the event kinematics automatically by the program [30]. An uncertainty of this calculation is estimated by the difference from an alternative calculation which uses a fixed scale. All calculations are subject to the experimental kinematic and isolation requirements [17]. Theoretical uncertainties are best estimated for the fixed-order NLO and NNLO calculations, where the scale uncertainties are well-defined. The estimation is done by increasing and decreasing the scale of each calculation by a factor of two relative to the default scale and, for the NLO PDF uncertainties, by using the 20 CTEQ6M eigenvectors [31].

The measured cross section for diphoton production integrated over the acceptance is $12.3 \pm 0.2_{\text{stat}} \pm 3.5_{\text{syst}}$ pb. The predictions for the integrated cross section are 12.4 ± 4.4 pb from SHERPA, 11.5 ± 0.3 pb from MCFM, and $11.8^{+1.7}_{-0.6}$ pb from the NNLO calculation. All predictions are consistent with the measurement. Figure 1 shows the comparisons between the observed and predicted diphoton distributions in mass M, transverse momentum P_T and azimuthal separation $\Delta\phi$ between the momenta of the two photons in the event.

All predictions for the mass distribution show a reasonable agreement with the data for all calculations above the maximum at 30 GeV/c^2, particularly in the region around $M=125$ GeV/c^2 relevant to measurements of the Higgs boson [7]. All predictions underestimate the data rate around and below the maximum, although the NNLO prediction reproduces better the data than the other two predictions. The SHERPA prediction tends to underestimate the data for $M>250$ GeV/c^2.

In the P_T spectrum, the MCFM prediction underestimates the data in the region between 30 and 60 GeV/c, a feature also observed in the earlier measurements [12, 25]. The other two predictions describe the data fairly well in this region. For $P_T<20$ GeV/c, where soft gluon radiation becomes important, only the SHERPA prediction provides a good description of the data because the parton showering provides an effective resummation of multiple soft-gluon emission amplitudes. The fixed-order predictions diverge in the limit of vanishing P_T. The NNLO prediction tends to overestimate the data rate for $P_T>60$ GeV/c.

Of special importance is the $\Delta\phi$ spectrum where all PS and NLO predictions examined in the previous papers failed to describe the data over the full range. The SHERPA model shows the best agreement at larger $\Delta\phi$, where the diphoton system acquires substantial transverse momentum due to multiple soft-gluon emission. However, SHERPA progressively underestimates the data rate below 1.5 rad. The NNLO calculation is the only prediction consistent with the data in the low $\Delta\phi$ tail, which contains photon pairs with very low mass and rel-

atively high P_T. This calculation tends to underestimate the data rate above 1 rad. The SHERPA and NNLO predictions generally are in better agreement with the data than MCFM. This shows that higher than NLO contributions, included in both calculations in different ways, are needed in order to better describe the data. More channels open at higher order, such as diphoton production associated with the emission of two final-state partons (2→4 channels), which enhance the event rate at high P_T and low $\Delta\phi$.

The observed cross section enhancements at very low diphoton mass ($M{<}30$ GeV/c^2), moderate diphoton transverse momentum ($30{<}P_T{<}60$ GeV/c) and low $\Delta\phi$ ($<$1 rad) are correlated. The events involved in this correlation have a topology of *same-side* diphotons recoiling against at least one hard jet. For some of the contributions the cross section is enhanced, such as when the two photons are emitted by the same parton and are, therefore, predominantly almost collinear. Enhanced contributions begin to appear in 2→3 subprocesses. The importance of 2→3 subprocesses was shown in the previous CDF measurement [14], where the inclusion of photons radiated in hard γ+jet events substantially improved the agreement of the PS calculation with the data with respect to the simple 2→2 diphoton calculation. These subprocesses are treated in different ways at different orders of approximation. At NLO, diphotons emitted from the same parton can only appear in the fragmentation components [25]. At NNLO such contributions can result directly either from 2→3 subprocesses, where a quark loop is included in the diphoton production amplitude, or from tree-level 2→4 subprocesses [29]. The SHERPA calculation also includes 2→4 subprocesses [30]. Thus NNLO and SHERPA describe the observed enhancement better than MCFM, which does not include such subprocesses.

In summary, the diphoton production cross section, differential in kinematic variables sensitive to the parton-level processes that govern the reaction, is measured using all data collected with the CDF II detector, corresponding to an integrated luminosity of 9.5 fb^{-1}. This measurement is consistent with the past CDF measurements [12, 14] and supersedes them. The measurement uses photons with $|\eta| < 1$ and has sufficiently high precision to resolve differences between state-of-the-art theoretical predictions. The results are compared with three calculations, which apply complementary techniques in predicting the cross section. The NNLO calculation is generally consistent with the data, although events with very low diphoton mass and high diphoton transverse momentum are not accurately described. The ME+PS SHERPA calculation is also consistent with the data except in the tails of the mass and the low $\Delta\phi$ distributions. Both NNLO and SHERPA describe the data better than the NLO MCFM calculation in regions sensitive to diphoton production channels resulting to nearly collinear photons. The comparisons show that parton-level processes of order higher than NLO, which was the standard approximation in older calculations, play an important role in diphoton production at the current level of experimental precision. This conclusion is supported by the findings of the recent ATLAS measurement at higher collision energy [15]. The inclusion of such processes in background calculations is thus important for high precision measurements of the recently discovered Higgs boson-like particle and searches for new phenomena in diphoton final states.

[1] T. Aaltonen *et al.* (CDF Collaboration), Phys. Rev. Lett. **103**, 061803 (2009); V. M. Abazov *et al.* (D0 Collaboration), Phys. Rev. Lett. **102**, 231801 (2009); G. Aad *et al.* (ATLAS Collaboration), arXiv:0901.0512 [hep-ex]; G. L. Bayatian *et al.* (CMS Collaboration), J. Phys. G **34**, 995 (2007).

[2] M. C. Kumar, P. Mathews, V. Ravindran, and A. Tripathi, Phys. Lett. B **672**, 45 (2009).

[3] V. M. Abazov *et al.* (D0 Collaboration), Phys. Rev. Lett. **104**, 241802 (2010).

[4] T. Aaltonen *et al.* (CDF Collaboration), Phys. Rev. D **83**, 011102 (2011).

[5] S. Mrenna and J. Willis, Phys. Rev. D **63**, 015006 (2001), and references therein.

[6] G. F. Giudice and R. Rattazzi, Phys. Rep. **322**, 419 (1999).

[7] G. Aad et al., ATLAS Collaboration, Phys. Lett. B 716 (2012) 1; S. Chatrchyan et al., CMS Collaboration, Phys. Lett. B 716 (2012) 30.

[8] C. Balazs, E. L. Berger, P. Nadolsky, and C.-P. Yuan, Phys. Lett. B **637**, 235 (2006); Phys. Rev. D **76**, 013009 (2007); Phys. Rev. D **76**, 013008 (2007).
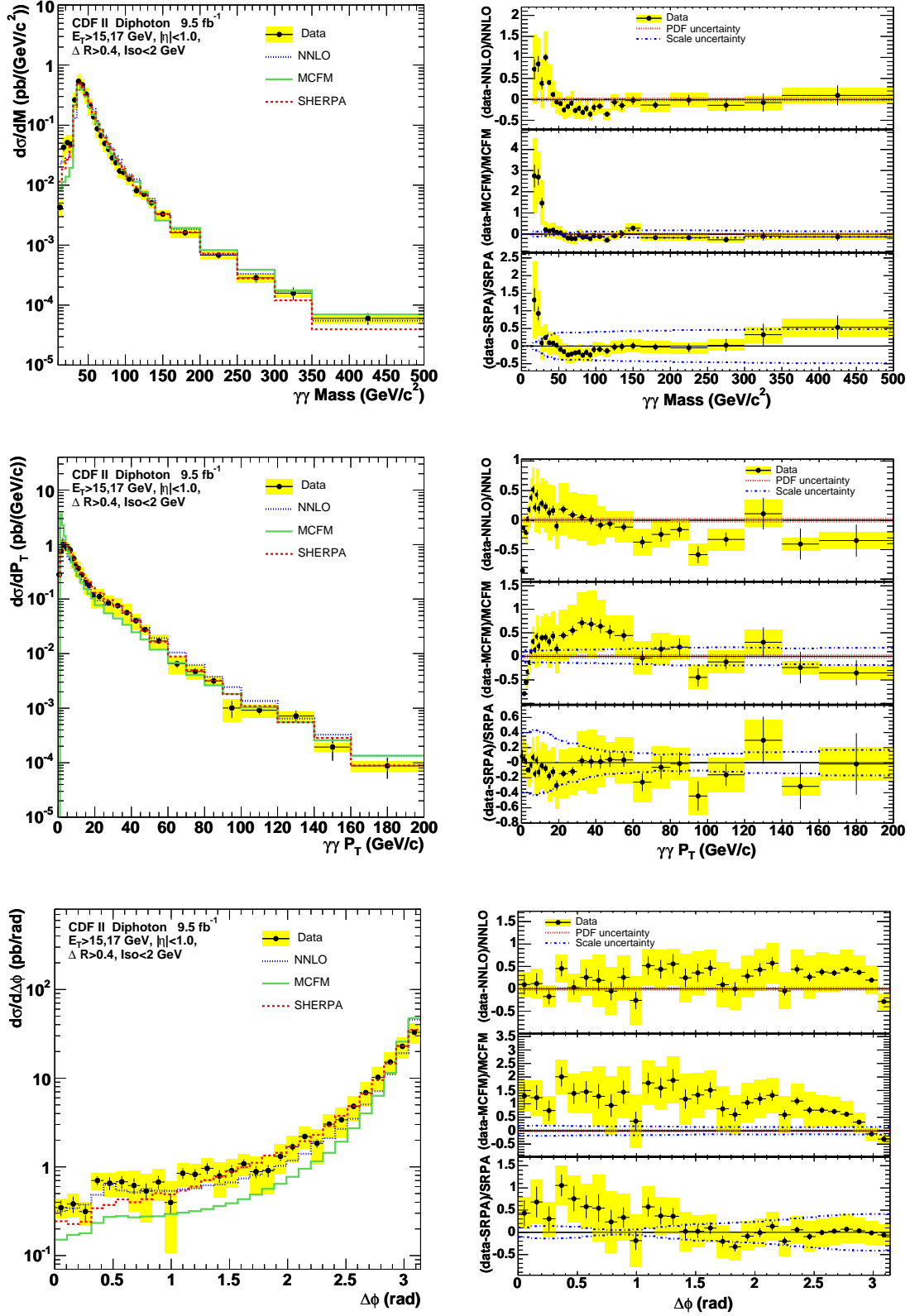
FIG. 1: Measured differential cross sections as functions of the diphoton mass (top) and transverse momentum (middle), and of the azimuthal difference between the photon directions (bottom), compared with three theoretical predictions discussed in the text. The left panels show the absolute comparisons. The lines show the predictions from SHERPA (dashed), MCFM (solid), and NNLO (dotted). The right panels show the fractional deviations of the data from the theoretical predictions. The lines show the scale uncertainty (dot-dashed) and the PDF uncertainty (dotted) of the predictions. The vertical axis scales differ between fractional-deviation plots. The shaded area around the data points indicates the total systematic uncertainty of the measurement.

[9] E. Bonvin *et al.* (WA70 Collaboration), Z. Phys. C **41**, 591 (1989); Phys. Lett. B **236**, 523 (1990).

[10] C. Albajar *et al.* (UA1 Collaboration), Phys. Lett. B **209**, 385 (1988).

[11] J. Alitti *et al.* (UA2 Collaboration), Phys. Lett. B **288**, 385 (1992).

[12] F. Abe *et al.* (CDF Collaboration), Phys. Rev. Lett. **70**, 2232 (1993); D. Acosta *et al.* (CDF Collaboration), Phys. Rev. Lett. **95**, 022003 (2005).

[13] V. M. Abazov *et al.* (D0 Collaboration), Phys. Lett. B **690**, 108 (2010).

[14] T. Aaltonen *et al.* (CDF Collaboration), Phys. Rev. Lett. **107**, 102003 (2011); Phys. Rev. D **84**, 052012 (2011).

[15] G. Aad *et al.* (ATLAS Collaboration), arXiv:1211.1913 [hep-ex], to be published in J. High Energy Phys.

[16] T. Aaltonen *et al.* (CDF Collaboration), Phys. Lett. B **717**, 173 (2012).

[17] All comparisons are summarized in the supplemental material of this Letter.

[18] CDF II Collaboration, FERMILAB-PUB-96/90-E (1996); see also A. Sill *et al.*, Nucl. Instrum. Methods A **447**, 1 (2000) and T. Affolder *et al.*, Nucl. Instrum. Methods A **526**, 249 (2004) for the spectrometer; L. Balka *et al.*, Nucl. Instrum. Methods A **267**, 272 (1988) and S. Bertolucci *et al.*, Nucl. Instrum. Methods A **267**, 301 (1988) for the central calorimeters.

[19] T. Aaltonen *et al.* (CDF Collaboration), Phys. Rev. D **82**, 052005 (2010).

[20] The calorimeter isolation is defined as the difference of the transverse energy in the isolation cone minus the transverse energy in the tower cluster of the photon. The isolation cone is defined to have a radius $R = \sqrt{(\Delta\eta)^2 + (\Delta\phi)^2} = 0.4$ around the axis of the shower profile. The isolation requirement implies that the angular separation of the two photons is $\Delta R \geq 0.4$.

[21] The track isolation is defined as the scalar sum of the transverse momenta $p_T = |\vec{p}| \sin\theta$ of all tracks originating from the primary vertex of the event and lying within the photon reconstruction cone.

[22] T. Sjöstrand, P. Eden, C. Friberg, L. Lombard, G. Miu, S. Mrenna, and E. Norrbin, Comp. Phys. Comm. **135**, 238 (2001); the version of PYTHIA used here is 6.2.16.

[23] E. Gerchtein and M. Paulini, CHEP-2003-TUMT005, arXiv:physics/0306031; the version of GEANT used for the detector simulation is 3.21, see the CERN Program Library Long Writeup W5013.

[24] S. Klimenko, J. Konigsberg, and T.M. Liss, FERMILAB-FN-0741 (2003).

[25] T. Binoth, J. P. Guillet, E. Pilon, and M. Werlen, Eur. Phys. J. C **16**, 311 (2000); Phys. Rev. D **63**, 114016 (2001).

[26] L. Bourhis, M. Fontannaz, and J. P. Guillet, Eur. Phys. J. C **2**, 529 (1998).

[27] J. M. Campbell and R. K. Ellis, Phys. Rev. D **60**, 113006 (1999). We use version 6.1 with the MSTW8NL parton distribution functions. The renormalization, factorization and fragmentation scales are set to half the diphoton invariant mass.

[28] A. Gehrmann-De Ridder, T. Gehrmann, E. W. N. Glover, and G. Heinrich, Eur. Phys. J. C **7**, 29 (1999).

[29] S. Catani, L. Cieri, D. de Florian, G. Ferrra, and M. Grazzini, Phys. Rev. Lett. **108**, 072001 (2012).

[30] T. Gleisberg, S. Höche, F. Krauss, M. Schönherr, S. Schumann, F. Siegert, and J. Winter, J. High Energy Phys. 02 (2009) 007. We use version 1.3.1 with the CTEQ6.6M parton distribution function.

[31] J. Pumplin, D. R. Stump, J. Huston, H. L. Lai, P. Nadolsky, and W. K. Tung, J. High Energy Phys. 07 (2002) 012.